Developmental Biology 375 (2013) 140–151

Contents lists available at SciVerse ScienceDirect

Developmental Biology

journal homepage: www.elsevier.com/locate/developmentalbiology

Hes1 in the somatic cells of the murine ovary is necessary for oocyte survival and maturation

Iris Manosalva [a,b,*], Aitor González [a,b,1], Ryoichiro Kageyama [a,b,*]

[a] Institute for Virus Research, Kyoto University, Kyoto, Japan
[b] Japan Science and Technology Agency, CREST, Kyoto, Japan

ARTICLE INFO

Article history:
Received 25 February 2012
Received in revised form
18 December 2012
Accepted 19 December 2012
Available online 27 December 2012

Keywords:
Mouse
Ovary
Notch pathway
Hes1
Oocytes
Fertility

ABSTRACT

The Notch pathway plays an important role in ovary development in invertebrates like Drosophila. However its role for the mammalian ovary is unclear. Mammalian *Hes* genes encode transcriptional factors that mediate many of the activities of the Notch pathway. Here, we have studied the function of *Hes1* during embryonic development of the mouse ovary. We find that Hes1 protein is present in somatic cells and oocyte cytoplasm and decreases between E15.5 and P0. Conventional *Hes1* knock-out (KO), *Hes1* conditional KO in the ovarian somatic, and chemical inhibition of Notch signaling decrease the total number, size and maturation of oocytes and increase the number of pregranulosa cells at P0. These defects correlate with abnormal proliferation and enhanced apoptosis. Expression of the proapoptotic gene *Inhbb* is increased, while the levels of the antiapoptotic and oocyte maturation marker Kit are decreased in the *Hes1* KO ovaries. Conversely, overactivation of the Notch pathway in ovarian somatic cells increases the number of mature oocytes and decreases the number of pregranulosa cells. Fertility is also reduced by either *Hes1* deletion or Notch pathway overactivation. In conclusion, our data suggest that the Notch–Hes1 pathway regulates ovarian somatic cell development, which is necessary for oocyte survival and maturation.

Introduction

The Notch pathway is crucial for tissue homeostasis and patterning in many organs (Andersson et al., 2011). It also plays an important role in the development of invertebrate follicles in *Caenorhabditis elegans* and *Drosophila melanogaster* (Klusza and Deng, 2011; Waters and Reinke, 2011). However, the role of the Notch pathway in the mammalian ovary development is still unclear.

The Notch proteins are one-transmembrane receptors that consist of an extracellular domain, a transmembrane domain and an intracellular domain (NICD). The Notch receptors are bound by Jagged and Delta ligands and modulated by Fringe glycosyltransferases (Andersson et al., 2011). Binding between ligand and receptor results in the cleavage of the NICD, translocation of NICD into the nucleus and binding to the Rbpj transcription factor for target gene activation. Among the target genes, the family of Hes transcription factors are important mediators of Notch signaling by repressing differentiation related genes (Kageyama et al., 2007).

The role of the Notch pathway in invertebrate oocyte development is relatively well understood. In *Drosophila*, germ cell-derived Delta activates the Notch receptor in the somatic follicle cells and regulates cell growth and exit from the mitotic cell cycle (Klusza and Deng, 2011). In *C. elegans*, Delta in the somatic cells activates the Notch receptor in the germline stem cells to regulate the balance between meiosis and mitosis (Waters and Reinke, 2011).

Murine oocyte development starts when primordial germ cells (PGC) originate from epiblast cells at embryonic day (E)7.5 and populate the gonads at around E10.5. At E13.5, somatic cells divide and surround the oocyte forming cysts (Pepling and Spradling, 1998). Between E13.5 and postnatal day (P)0, oocytes grow and progress through different stages of prophase I (Speed, 1982). Between E18.5 and P0, the majority of oocytes are depleted by apoptosis, possibly by some selection process (Ghafari et al., 2007).

The mouse oocytes express the Notch ligand *Jag1* whereas ovarian somatic cells express the Notch receptors Notch2 and Notch3, the glycosyltransferase Lunatic Fringe (Lfng) and the downstream transcriptional effector Hes1 among other Notch pathway genes (Johnson et al., 2001; Hahn et al., 2005). Functional studies have shown that chemical inactivation of the Notch pathway in explant newborn ovaries results in follicles

* Corresponding authors at: Institute for Virus Research, Kyoto University, Kyoto, Japan.
E-mail addresses: immp6@yahoo.com (I. Manosalva), rkageyam@virus.kyoto-u.ac.jp (R. Kageyama).
[1] Present address: Institut de Génétique et de Biologie Moléculaire et Cellulaire (IGBMC), CNRS (UMR 7104), Inserm U964, Université de Strasbourg, Illkirch, France.

0012-1606/$ - see front matter © 2012 Elsevier Inc. All rights reserved.
http://dx.doi.org/10.1016/j.ydbio.2012.12.015

containing more than one oocyte (multi-oocyte follicles) (Trombly et al., 2009). Multi-oocyte follicles, abnormal meiosis and reduced fertility have been also reported in the *Lfng* knock-out (KO) mice (Hahn et al., 2005). In addition, ovarian cancer cells show abnormal expression of Notch pathway genes, and their growth and apoptosis can be controlled with chemical inhibitors of the Notch pathway (Hopfer et al., 2005; Wang et al., 2010). Despite these studies, the exact function of Notch signaling in the ovary remains to be determined.

To investigate the function of the Notch pathway for the mammalian ovary development, we analyzed conventional and somatic cell-specific *Hes1* KO ovaries as well as somatic cell-specific overactivation of the Notch pathway in the ovary. Our results suggest that *Hes1* in the somatic cells supports oocyte maturation and survival at P0. These data uncover a new role of the Notch pathway for the mammalian ovary development.

Materials and methods

Animals

The presence of vaginal plug was considered as day 0.5 of gestation. Genotyping was carried out as previously described: *Hes1* KO (Ishibashi et al., 1995), *Hes1* flox (Imayoshi et al., 2008), *Amhr2*-cre (Jamin et al., 2002), TNAP-Cre (Lomelí et al., 2000), and ROSA-NICD (Murtaugh et al., 2003). All experiments were carried out at postnatal day 0 (P0) unless indicated otherwise. All animals were handled in accordance with the Kyoto University Guide for the Care and Use of Laboratory Animals.

In situ hybridization and real-time PCR

In situ hybridization was carried out using the mouse *Hes1* probe as previously described (Imayoshi et al., 2008). For real-time PCR, RNA was isolated from ovaries using the standard Trizol procedures. Reverse transcription reaction and quantitative PCR were performed with ReverTraAce and SYBR Green (Toyobo), respectively. Real-time PCR measurement and normalization were carried out as previously described (Kobayashi et al., 2009). Gapdh, which does not change in the *Hes1* KO samples, was used as housekeeping (supplementary Fig. S1). Primers are shown in supplementary Table S1.

Immunohistochemistry

For immunohistochemistry of cryosections, samples were included in OCT, cut (10 μm), postfixed in formalin for 10 min and then washed in PBS for 5 min (3 times). Antigen retrieval (0.01M sodium citrate buffer, 10 min at 100 °C) was performed for all antibodies with the exception of Pecam1 and Ngfr. Sections were washed in PBS and blocked (5% serum and 0.1% Triton X-100 in PBS) for 2 h at room temperature. Primary antibodies were diluted in the blocking solution and incubated overnight at 4 °C. Secondary antibodies and DAPI were incubated for 1 h at room temperature. Primary antibodies and dilution rates were as follows: cleaved Caspase 3 (1:100, Cell Signaling #9661), Ki67 (1:100, BD Pharmingen #556003), Kit (1:100, Calbiochem #961–976), Hes1 (1:200, Kobayashi et al. (2009)), Ngfr (1:100, Promega G323A), Pecam1 (1:100, BD Pharmingen #550274), Sycp3 (1:100, Abcam ab15092), and Tra98 (1:1000, B-Bridge #73-003). For immunohistochemistry of paraffin sections, embryos were fixed in 4% PFA, overnight at 4 °C, paraffin embedded and sectioned (10 μm). Deparaffinized sections were subjected to antigen retrieval, endogenous peroxidase quenching, blocking and incubation with primary antibody (1:200, Hes1, Kobayashi et al. (2009)), and Foxl2 (1:200, NB100-1277). Detection was carried out with biotinylated secondary antibodies of the VECTASTAIN ABC kit. Slides were developed using DAB. As positive and negative controls for the Hes1 antibody, we show nuclear immunohistochemistry staining in WT fibroblasts and absent staining in *Hes1* KO fibrablasts and ovaries (supplementary Fig. S2A and B).

Bromodeoxyuridine (BrdU), Tunel and luciferase assays

For the BrdU assay, pregnant mice received a single injection of BrdU (50 μg/kg, BD Biosciences #347580) at E15.5 and E18.5, 2 h before collection. Ovaries were treated similarly as for immunofluorescence (see below) except that the antigen retrieval step was substituted by a treatment with DNAse I (Roche Diagnostic) for 60 min at 37 °C. For the Tunel assay, paraffin sections were deparaffinized and rehydrated. The Tunel protocol was taken from the instructions provided by the kit (Chemicon International). The luciferase assay was carried out as previously described using C3H10T1/2 cells in 10% FBS/DMEM and Lipofectamin LTX/Plus (Invitrogen) transfection reagent (Masamizu et al., 2006).

Ovary culture

Ovary culture was carried out as previously described with small variations (Tang et al., 2008). Ovaries from E17.5 CD-1 mice were dissected, bursal sac was removed in PBS and ovaries were put in 0.4-μm floating filters (Millicell-CM; Millipore Corporation, Billerica, MA) and cultured for 4 days at 37 °C in a chamber containing 5% CO2. Medium DMEM-F12 suplemented with 0.1% Albumax (Invitrogen), penicillin–streptomycin (Invitrogen), 0.1% BSA (Sigma), 27.5 μg/ml transferrin (Sigma), and 0.05 mg/ml l-ascorbic acid (Sigma). Treatments were DAPT dissolved in DMSO (20 μM, Calbiochem) and recombinase Inhibin b (100 ng/ml, R&D Systems 659-AB). Cultured ovaries follow the histology treatment of the RT-PCR described before.

Oocyte collection

To retrieve MII-arrested oocytes, mice were superovulated by intraperitoneal injection of 5 IU PMSG followed by 5 IU hCG 48 h later. Cumulus enclosed oocytes complexes were collected from the ampulla of oviducts 13 h after hCG injection, placed in M2 medium, and freed of cumulus cells with 1 mg/ml hyaluronidase. DAPI staining was carried out after fixing the MII oocytes with 4% PFA for 5 min. Fluorescence was captured with a confocal scaning system.

Quantification and statistical analysis

We counted the total number of positive cells from sections (30 μm apart) of the entire ovary and rescaled it with the WT number. For quantification of the Pecam1 signal, the Pecam1 color channel was binarized and the positive area percentage was computed with ImageJ (NIH, Bethesda, USA). All experiments were carried out in 3 or more animals unless indicated otherwise. To calculate statistical significance, differences between control and mutant populations were evaluated with Student's *t* test. A *P*-value less than 0.05 was considered significant.

Results

Hes1 expression dynamics in the fetal ovary

We first investigated the expression dynamics of *Hes1* in the fetal ovary. We carried out in situ hybridization with a probe for

Hes1 mRNA and found that *Hes1* mRNA is expressed in the ovary at E15.5 at low levels and further decreases at E17.5 (Fig. 1A). Real-time PCR with *Hes1* primers in cDNA samples from ovaries at E15.5, E17.5 and P0 stages also showed low levels of *Hes1* mRNA expression that decreased with increasing age (Fig. 1B). We also investigated the levels of Hes1 protein at different stages by immunohistochemistry. At E15.5, many ovarian cells show low levels of Hes1 protein staining (left column in Fig. 1C). From this stage on, Hes1 protein progressively decreased at E17.5 and P0 stages (left column in Fig. 1C). Hes1 and Tra98 immunohistochemistry signals did not overlap suggesting that Hes1 was absent from the oocyte nuclei (middle and right columns in Fig. 1C). Higher magnification images showed that Hes1 protein is present in the oocyte cytoplasm and in the nuclei of surrounding somatic cells at P0 stage (supplementary Fig. S3) (Trombly et al., 2009).These data suggest that *Hes1* mRNA expression decreases between E15.5 and P0, and that Hes1 protein is mainly present in oocyte cytoplasm and somatic cells.

Hes1 expression is known to oscillate in different tissues like the presomitic mesoderm, neuronal precursors and embryonic stem cells (Masamizu et al., 2006; Shimojo et al., 2008; Kobayashi et al., 2009). To investigate whether Hes1 also oscillates in the ovary, we monitored the luminescence of trypsinized ovary cells from mice carrying a *Hes1* promoter luciferase reporter (Masamizu et al., 2006). *Hes1* expression was found to oscillate in ovary cells with a period of about 3–6 h (supplementary Fig. S4).

Fewer and smaller oocytes and more pregranulosa cells in the absence of Hes1

To investigate the function of *Hes1*, we examined the ovary of conventional *Hes1* KO mice (Ishibashi et al., 1995), some of which survived until just after birth. Externally, the mutant ovaries were similar to the control (supplementary Fig. S5). However, histological analysis showed that grown follicles were present in the wild-type (WT) but absent in the mutant ovaries at P0 (Fig. 2A).

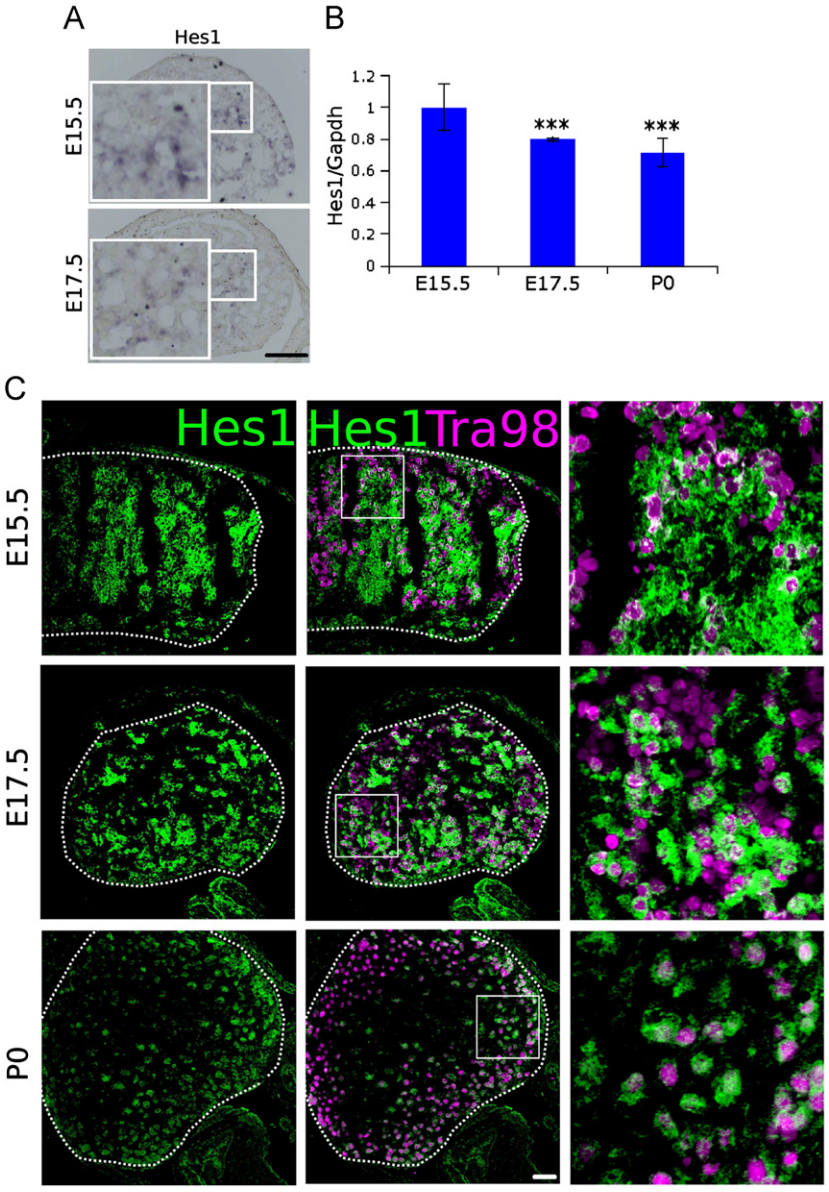

Fig. 1. *Hes1* expression dynamics and localization in fetal ovaries. (A,B) *Hes1* mRNA expression by in situ hybridization ($n=2$) (A) and real-time PCR (B). *Hes1* mRNA is expressed at low levels and decreases between embryonic stages E15.5 and birth. (C) Double immunohistochemistry of Hes1 protein and the oocyte marker Tra98. Hes1 protein is stained at low levels (contrast increased to show more detail) and decreases between E15.5 and P0 (left column). Hes1 and Tra98 immunohistochemistry signals do not colocalize suggesting that Hes1 is excluded from oocyte nuclei. Boxed regions are enlarged in the third column. Scale bars: 50 μm; $^{***}P<0.001$.

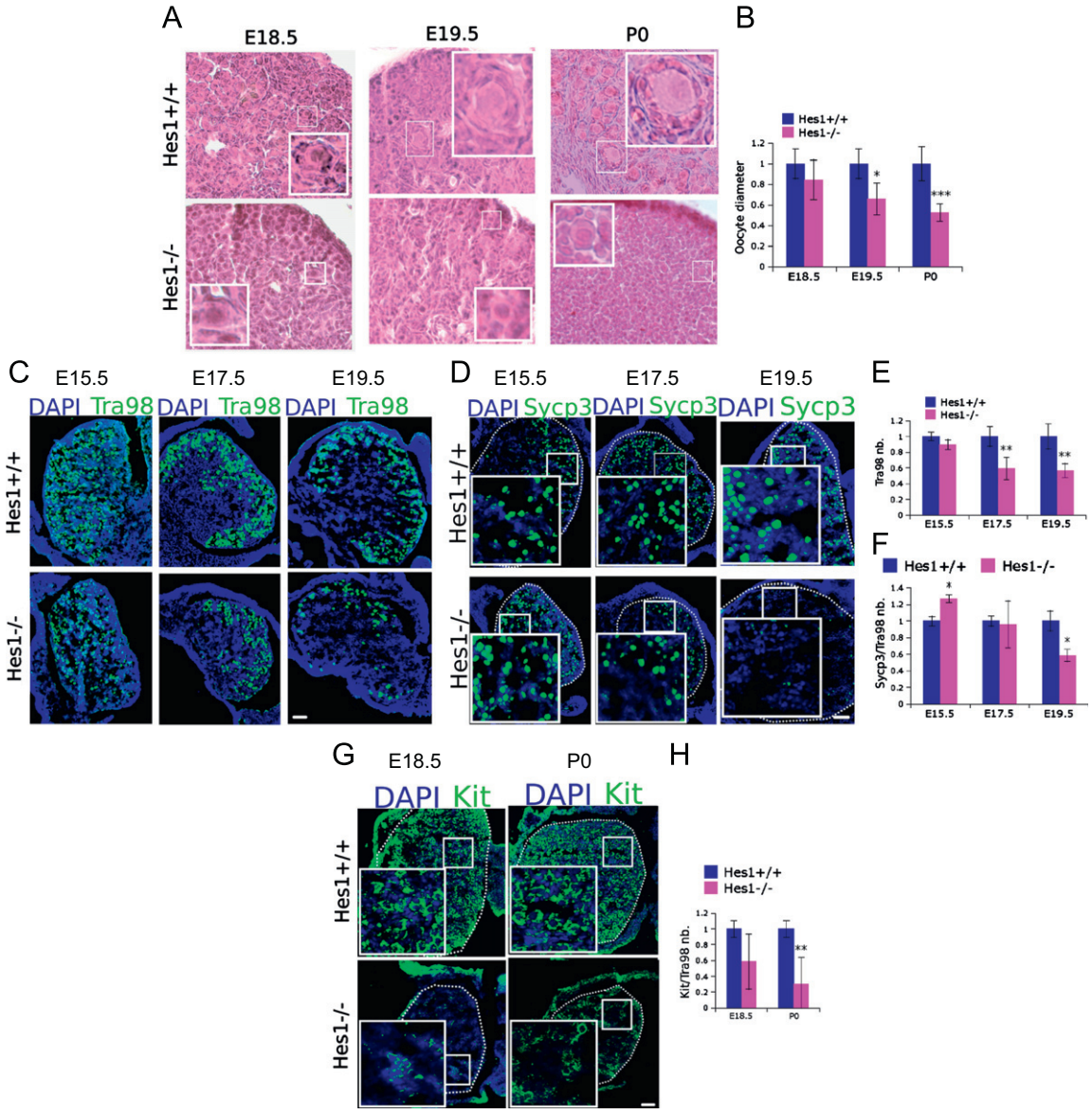

Fig. 2. The number and diameter of oocytes are reduced in the *Hes1* KO mice. (A,B) Hematoxilin staining of ovaries at E18.5, E19.5 and P0 stages in the *Hes1* KO and quantification. Grown oocytes are rare at E19.5 and absent at P0 in *Hes1* KO ovaries. Quantification shows a diameter decrease to about 60% after E19.5 (B). (C–H) Immunofluorescence and quantification of the oocyte marker Tra98 (C,E), the meiosis marker Sycp3 (D,F) and the mature oocyte marker Kit (G,H). Oocytes marked by Tra98 decrease in number since E17.5 in the Hes1 KO to about 50% (C,E). The ratio of Sycp3/Tra98 oocytes, which represents meiotic oocytes, decreases to about 60% at E19.5 (D,F). The ratio of Kit/Tra98 oocytes, which represents mature oocytes, strongly decreases after E18.5 (G,H). Boxed regions are enlarged in the corners. Scale bars: 50 μm; $^{*}P < 0.05$, $^{**}P < 0.01$, $^{***}P < 0.001$.

Quantification of the oocyte size showed a 30% lower diameter at E19.5 and a 50% lower diameter at P0 (Fig. 2B). We also examined the number of oocytes by immunohistochemistry with the oocyte marker Tra98. The number of oocytes in the mutants was comparable to the WT at E15.5 but decreased to about 60% at E17.5 and thereafter (Fig. 2C and E). Chromosomal defects could not be detected (supplementary Fig. S6), but oocytes in meiosis decreased to about 60% at E19.5 as evaluated by the meiotic marker Sycp3 (Fig. 2D and F). Mature oocytes, which are labeled by the Kit antibody, also decreased at P0 (Fig. 2G and H). Real-time PCR of ligand *Kitl* and receptor *Kit* also showed lower expression at P0 (supplementary Fig. S7). These data suggest that the number and maturation of oocytes are decreased in *Hes1* mutant ovaries.

We next examined whether differentiation of ovarian somatic cells also changes in the absence of *Hes1*. For this purpose, we carried out immunohistochemistry with different markers of ovarian somatic cells. Immunohistochemistry of the pregranulosa cell marker Foxl2 showed that the number of pregranulosa cells increases in *Hes1* KO ovaries at E15.5 and E18.5 (Fig. 3A and B). *Foxl2* expression levels at E17.5 were also increased as evaluated by real-time PCR (Fig. 3C). Other somatic markers like *Fst* and *Rspo1* also increased in the *Hes1* KO ovaries (Fig. 3C). However, the pregranulosa precursor marker *Lhx9* decreased in the *Hes1* KO ovary (Fig. 3C). We also examined other somatic cell types in the *Hes1* mutant ovaries, namely medulla and endothelial cells. We used Ngfr as a marker of medulla (stroma) cells (Uda et al., 2004). Immunofluorescence of the medulla marker Ngfr decreased in the *Hes1* KO ovaries (Fig. 3D). On the other hand, the area percentage of the endothelial cell marker Pecam1 increased at E15.5 but decreased at E19.5 (Fig. 3E and F). These data suggest that pregranulosa cells increase in the *Hes1* KO ovaries, while other somatic cell types decrease. The equivalent cell type of pregranulosa cells in the testis are Sertoli cells, which express *Fgf9*, *Pdgfa*

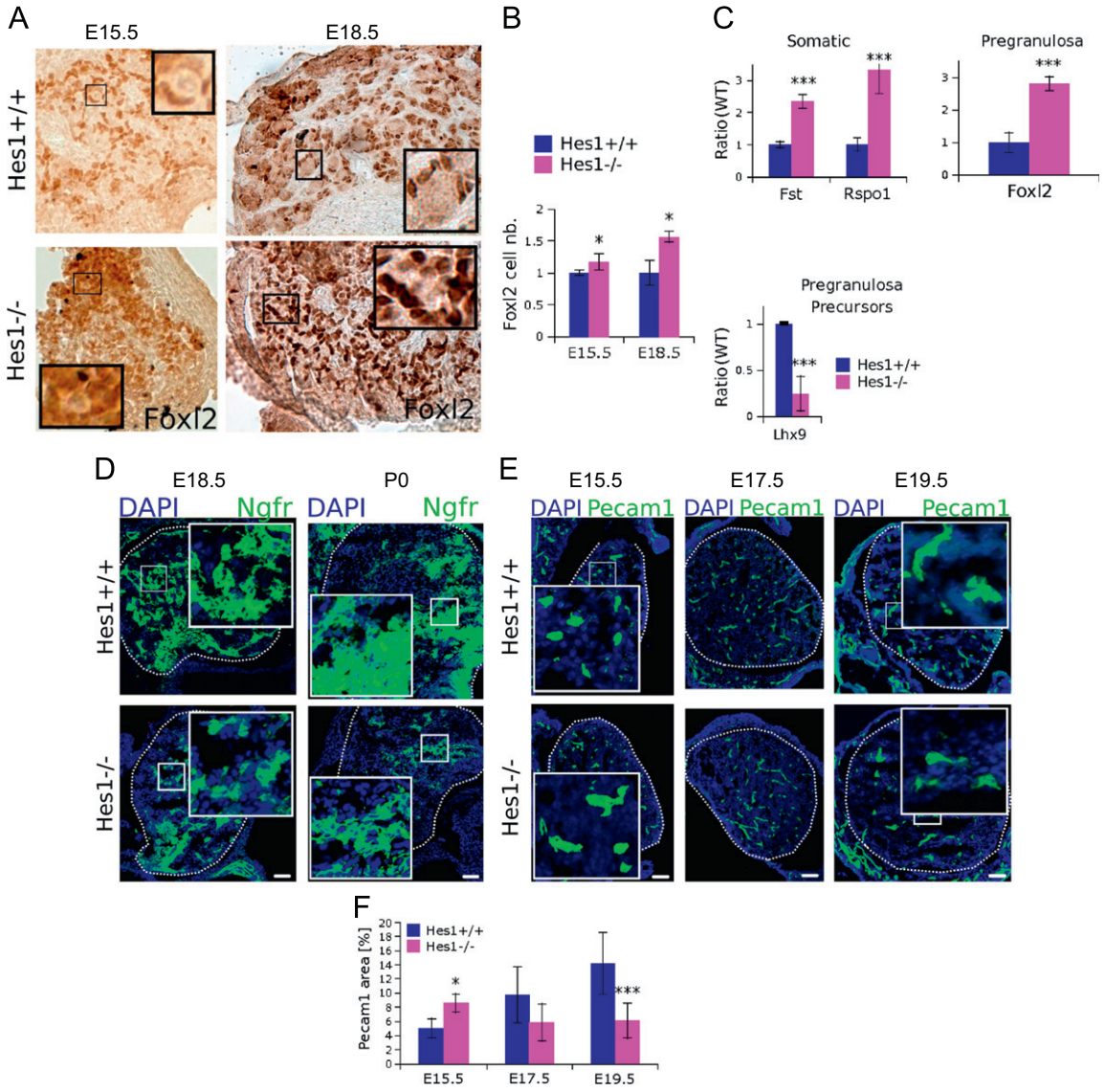

Fig. 3. The number of pregranulosa cells increases but medulla and endothelial cells decrease in the *Hes1* KO mice. (A,B) Immunohistochemistry of the pregranulosa cell marker Foxl2 at E15.5 and E18.5 stages. The number of Foxl2 positive cells increases in the *Hes1* KO at E15.5 and E18.5. (C) Expression of the somatic cell makers Fst and Rspo1, the pregranulosa cell marker *Foxl2* and the pregranulosa precursor cell marker Lhx9 in the *Hes1* KO by real-time PCR at E17.5. The mRNA expression levels of somatic cell markers increase in the *Hes1* KO. (D) Immunofluorescence of the medulla cell marker Ngfr in mutant ovaries. The fluorescence of the medulla cell marker Ngfr decreases in the mutant ovaries at E18.5 and P0 embryonic stages. (E,F) Immunofluorescence of the endothelial cell marker Pecam1 in *Hes1* KO ovaries and quantification. The levels of the endothelial cell marker Pecam1 increase at E15.5 but decrease at E19.5. Boxed regions are enlarged in the corners. Scale bars: 50 μm; $^{*}P < 0.05$, $^{**}P < 0.01$, $^{***}P < 0.001$.

and *Sox9*. Real-time PCR with primers for these genes in female mutant ovaries showed an increase of *Fgf9* and *Sox9* (supplementary Fig. S8). By contrast, expression of markers of male leydig cells and interstitial cells decreased in the mutant ovaries (supplementary Fig. S8). These observations suggest that *Hes1*-null pregranulosa cells have mixed features of testicular Sertoli cells. In conclusion, *Hes1* deletion in the ovary results in lower number, size and maturation of oocytes, and higher number of pregranulosa cells.

Abnormal cell number in the Hes1 KO ovaries might arise from altered proliferation and enhanced apoptosis

We then wanted to know whether the higher number of Foxl2 positive cells observed in the *Hes1* KO ovaries is associated with altered proliferation. Therefore, we analyzed proliferation in the ovary by immunohistochemistry with Ki67. Ki67 is strongly expressed in somatic cells and weakly in oocytes, but we focused on the strong somatic cell expression. Comparison of mutant and WT ovaries showed more Ki67 positive cells at E15.5 and less at E18.5 (Fig. 4A and C). We also carried out the BrdU incorporation assay that labels the S-phase of the cell cycle. Immunohistochemistry with the BrdU antibody showed that BrdU incorporation is enhanced at E15.5 and reduced at E18.5 (Fig. 4B and D). These data suggest that proliferation is enhanced at E15.5 and reduced at E18.5. We also examined the expression of cell cycle inhibitors *Cdkn1c* and *Gadd45g* by real-time PCR in cDNA samples synthesized from WT and *Hes1* KO ovaries. Our data show that Cdkn1c decreases at E15.5 and increases at E18.5, while Gadd45g increases at E18.5 in agreement with the Ki67 and BrdU results (Fig. 4E).

We also wanted to know the cause for the lower number of oocytes in the *Hes1* KO ovaries, so that we examined apoptosis by Caspase3 immunohistochemistry and Tunel assay. Double

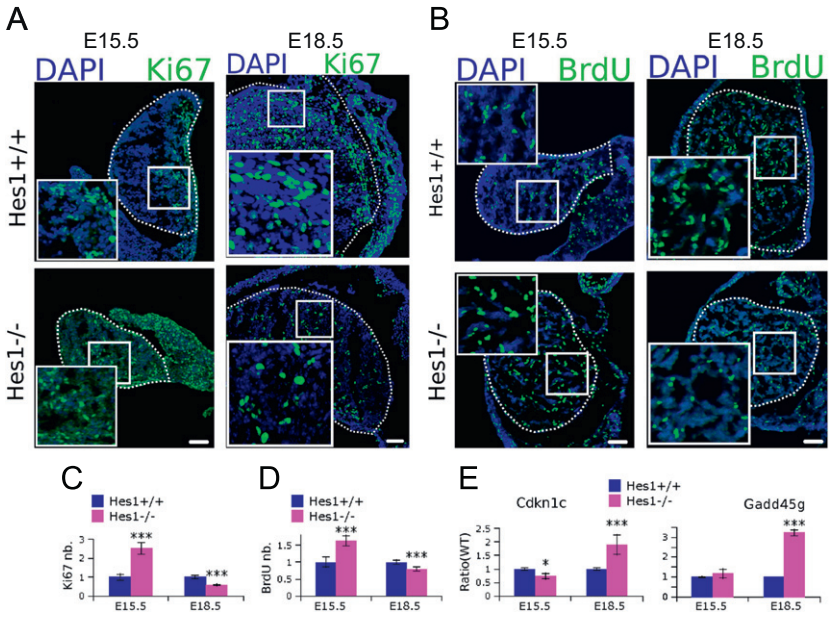

Fig. 4. Proliferation is increased at E15.5 and decreased at E18.5 in the *Hes1* KO ovaries. (A,C) Ki67 immunofluorescence in the *Hes1* KO ovaries at E15.5 and E18.5 and quantification. The number of Ki67 labeled cells increases at E15.5 and decreases at E18.5. (B,D) BrdU immunofluorescence in the *Hes1* KO ovaries at E15.5 and E18.5 and quantification. The number of cells incorporating BrdU increases at E15.5 and decreases at E18.5. (E) Expression of the cell cycle inhibitor genes *Cdkn1c* and *Gadd45g* by real-time PCR. The expression of *Cdkn1c* decreases at E15.5. Later at E18.5, the expression of both *Cdkn1c* and *Gadd45g* increases at E18.5. Boxed regions are enlarged in the corners. Scale bars: 50 μm; $^{*}P<0.05$, $^{***}P<0.001$.

immunohistochemical staining of Tra98 and Caspase3 showed a higher number of oocytes in apoptosis at E15.5 and E19.5 (Fig. 5A and B). The Tunel assay also showed an increase of apoptosis from E16.5 onward in the mutant samples (Fig. 5C and D). Higher magnification images suggested that the Tunel signal stained oocyte nuclei. It was previously shown that ovarian apoptosis can be induced by *Inhbb* expression (Liu et al., 2010). Therefore, we measured the mRNA levels of *Inhbb* in *Hes1* KO ovaries by real-time PCR. *Inhbb* expression strongly increased in the *Hes1* KO ovaries at E18.5 and P0 (Fig. 5E). *Hes1* usually acts as a transcriptional repressor, so that one possibility is that Hes1 directly represses the *Inhbb* promoter (Kageyama et al., 2007). To evaluate this possibility, we carried out the luciferase assay after contransfection of an *Inhbb* promoter reporter and a *Hes1* expression plasmid in cultured cells (Dykema and Mayo, 1994). Our results show that Hes1 is able to repress the *Inhbb* promoter (supplementary Fig. S9). It was also observed that *Inhbb* expression is upregulated in Wnt4 mutants (Liu et al., 2010). Therefore, it is possible that *Wnt4* expression is decreased in the *Hes1* KO ovaries and this upregulates *Inhbb* expression. Indeed, we found by real-time PCR that *Wnt4* expression is decreased in the *Hes1* KO ovaries (supplementary Fig. S10). To further investigate whether Inhbb causes oocyte decrease through apoptosis, we cultured E17.5 WT ovaries with recombinant Inhbb for 4 days and examined oocyte number and apoptosis. We found that Inhbb treatment induces a non-significant decrease of oocyte number (Fig. 5F and G). Furthermore, double Tra98/Caspase3 immunohistochemistry showed a higher number of oocytes associated with Caspase3 staining (Fig. 5F and H). These results suggest that *Hes1* is necessary to decrease oocyte apoptosis and one possible mechanism is the repression of *Inhbb*.

Chemical inhibition of the Notch pathway decreases the size of oocytes and induces oocyte apoptosis

In several tissues, the *Hes1* promoter is activated by the Notch pathway (Kageyama et al., 2007). To check the requirement of the Notch pathway for *Hes1* promoter activation, we monitored the luminescence of ovaries carrying a *Hes1* promoter luciferase reporter in the presence of the chemical inhibitor DAPT. In the control experiment, the *Hes1* promoter reporter luminescence remained constant for at least 7 h, whereas in the presence of DAPT, *Hes1* rapidly decreased (supplementary Fig. S11). We also checked the levels of Hes1 protein by immunohistochemistry after culturing ovaries with DAPT for 4 days. Our results show that Hes1 protein levels are decreased by DAPT (supplementary Fig. S2C). Because DAPT downregulates the Hes1 protein levels in the ovary, we hypothesized that this inhibitor might induce some of the phenotypes of the *Hes1* KO. To test this hypothesis, we cultured explant ovaries at E17.5 for 4 days in the presence of DAPT. Oocytes in the DAPT-treated ovaries were smaller than the control (Fig. 6A). Quantification of the oocyte size showed that the average diameter decreases by around 30% (Fig. 6B). Immunohistochemistry with the oocyte marker Tra98 exhibited a 10% decrease of the oocyte number (Fig. 6C and D). Immunostaining of Caspase3 showed a 5-fold increase of apoptosis in the treated sample (Fig. 6C and E). Furthermore, *Inhbb* expression was increased by the DAPT-treatment (Fig. 6F). We also examined the number of pregranulosa cells marked by Foxl2 and found a higher number of these cells (Fig. 6G and H). These results suggest that the Notch pathway is necessary for *Hes1* expression, which prevents apoptosis and supports oocyte growth.

Conditional KO of Hes1 in somatic cells decreases the number and maturation of oocytes

To find out whether *Hes1* functions in germ cells, we crossed a TNAP-Cre line with the floxed *Hes1* line to generate oocyte specific *Hes1* conditional KO (cKO) mice (Lomelí et al., 2000; Imayoshi et al., 2008). Histological analysis of these mice did not show significant differences of the oocyte size (supplementary Fig. S12). We also crossed the TNAP-Cre line with a floxed *Rbpj* allele to generate oocyte specific *Rbpj* cKO mice (Han et al., 2002). We analyzed these ovaries for oocyte, somatic cell and endothelial cell number using Tra98, Cx43 and Pecam1 markers. In this experiment, we did not find any difference between control and mutant ovaries (supplementary

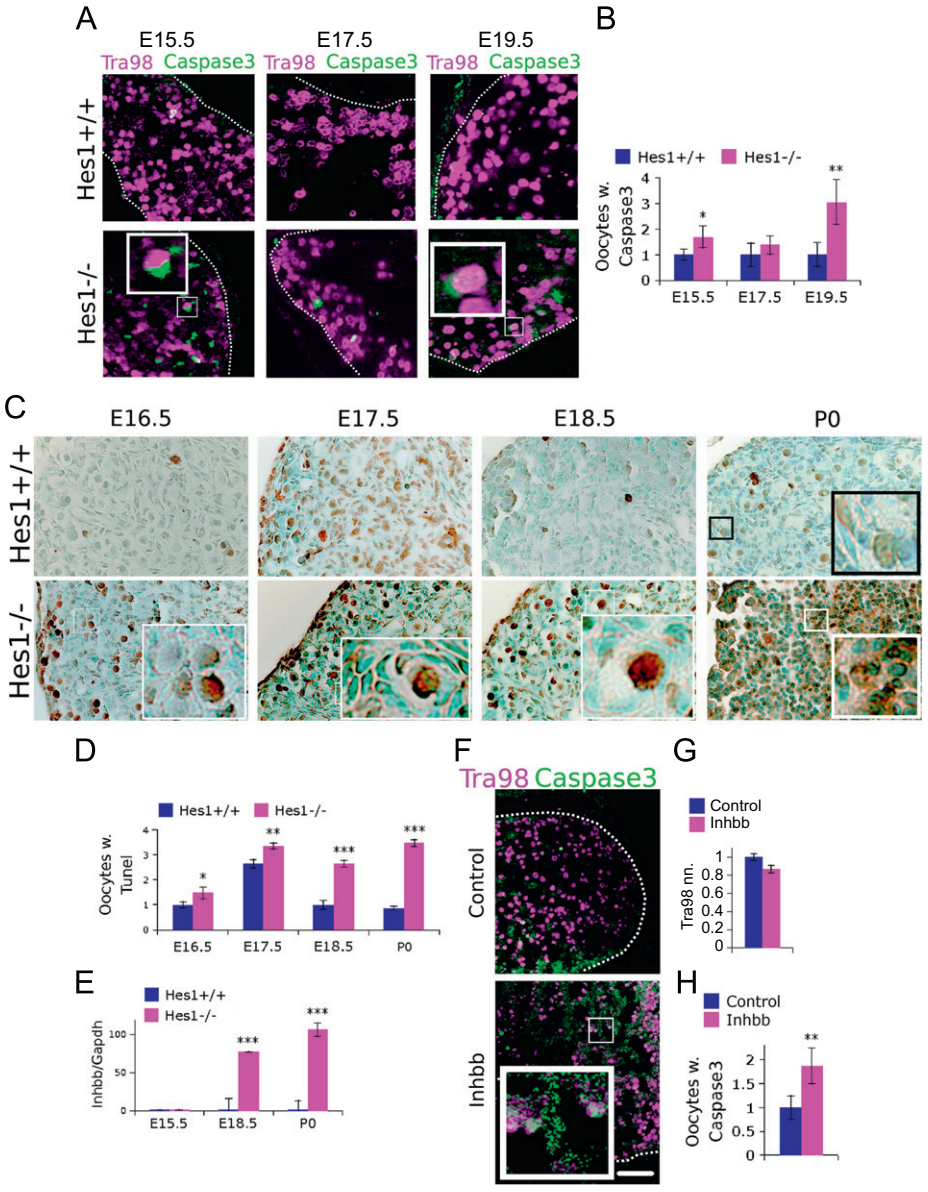

Fig. 5. Apoptosis increases in the *Hes1* KO ovaries. (A,B) Caspase3 immunofluorescence at E15.5, E17.5 and E19.5 and quantification. The number of oocytes with Caspase3 signal increases at E15.5 and E19.5. (C,D) Tunel staining at E16.5, E17.5, E18.5 and P0 and quantification. The number of oocytes marked by Tunel increases at all stages. (E) *Inhbb* expression by real-time PCR in the Hes1 KO ovaries. The expression of *Inhbb* increases strongly in the *Hes1* KO ovaries. (F–H) Double immunofluorescence of Caspase3 and Tra98 in ovaries cultured with Inhbb and quantification. The number of Tra98-positive oocytes exhibits a non-significant decrease (G), while the number of Caspase3-labeled oocytes increases in the Inhbb-treated ovaries (H). Boxed regions are enlarged in the corners. Scale bars: 50 μm; $^{*}P<0.05$, $^{**}P<0.01$, $^{***}P<0.001$.

Fig. S13). These data suggest that the Notch pathway does not play an important role in oocytes for fetal ovary development.

Next, we examined the function of *Hes1* in ovarian somatic cells by using an *Amhr2*-cre mouse line that induces Cre mediated recombination in almost all somatic cells of the ovary since E13.5 (Jamin et al., 2002). This mouse was crossed with *Hes1* flox mice to conditionally delete *Hes1* in ovarian somatic cells (*Hes1* cKO). First we checked whether the *Hes1* allele was deleted in the *Hes1* cKO by carrying real-time PCR and immunohistochemistry of Hes1. Our results show a drastic decrease of *Hes1* mRNA and protein expression in the *Hes1* cKO suggesting that the *Hes1* allele is deleted (supplementary Figs. S1B and S2D). The presence of some Hes1 staining in the Hes1 cKO could be due to incomplete recombination. Next, we examined these ovaries at P0 stage. Histological analysis showed that oocytes in the somatic *Hes1* cKO ovaries appeared smaller than the control (Fig. 7A). Quantification showed that the diameter of mutant oocytes decreases to around 50% (Fig. 7B). Then, we examined the number of oocytes by Tra98 immunofluorescence and found that the mutant ovaries had around 60% fewer oocytes than the control ovaries (Fig. 7C and D). The number of meiotic oocytes labeled by Sycp3 did not change (data not shown). Mature oocytes labeled with Kit antibody decreased to 80% in the mutant ovaries (Fig. 7E and G). Pregranulosa cells labeled by Foxl2 antibody presented a tendency to a higher number of cells in the *Hes1* cKO ovaries (Fig. 7F and H). By contrast, the medula cell marker Ngfr slightly decreased in the *Hes1* cKO ovaries (Fig. 7I). The endothelial cell marker Pecam1 did not show significant differences (data not shown). Thus, inactivation of *Hes1* in somatic cells recapitulated some of the ovary defects in the conventional *Hes1* KO mice, suggesting that *Hes1* in the somatic cells is important to regulate the oocyte number and maturation.

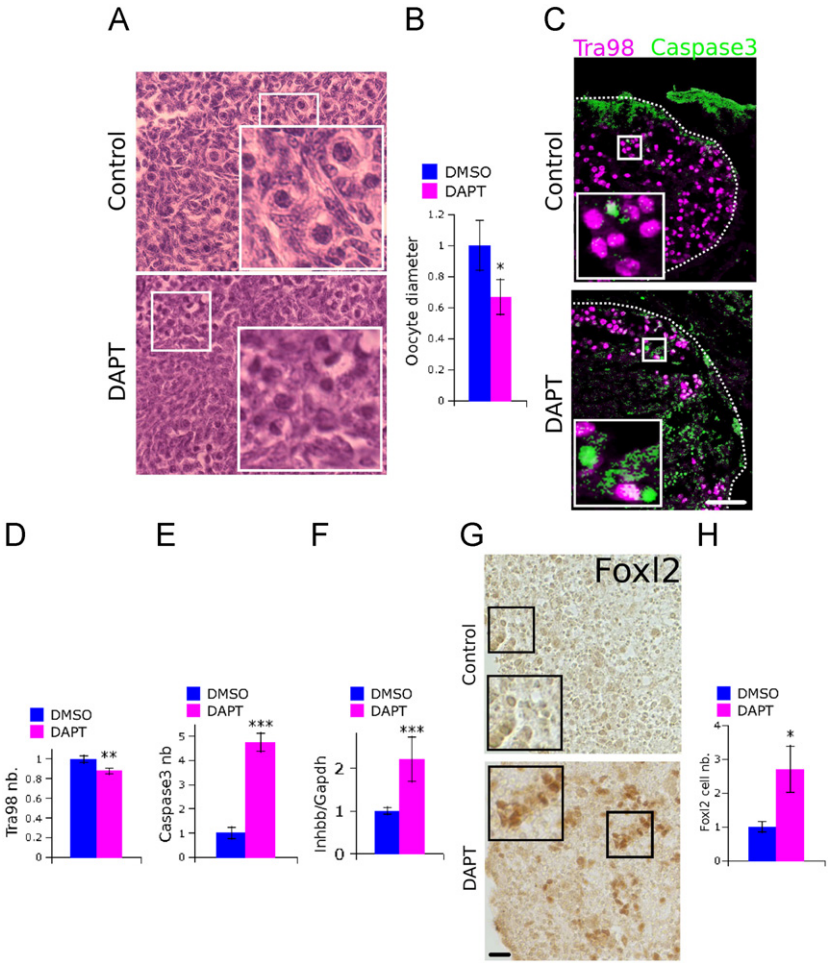

Fig. 6. The gamma-secretase inhibitor DAPT inhibits growth and induces apoptosis of oocytes. E17.5 ovaries were cultured for 4 days in the presence of DMSO or 20 μM DAPT. (A,B) Hematoxilin staining of ovary paraffin sections. In the DAPT-treated ovaries, the average diameter is about 25% smaller (B). (C–E) Double immunofluorescence of the oocyte marker Tra98 and the apoptosis marker Caspase3 and quantification. The number of oocytes decreases by about 10% (D), while the number of cells in apoptosis increases about 5-fold (E). (F) Expression of *Inhbb* in ovaries treated with DAPT as evaluated by real-time PCR. The levels of *Inhbb* mRNA increases in DAPT-treated ovaries. (G,H) Immunohistochemistry of the pregranulosa cell marker Foxl2 and quantification. The number of Foxl2 positive cells increases. Boxed regions are enlarged in the corners. Scale bars: 50 μm; $^{*}P<0.05$, $^{**}P<0.01$, $^{***}P<0.001$.

Overactivation of NICD in somatic cells increases the maturation of oocytes

If the role of the Notch pathway is mediated by *Hes1*, we would expect that Notch overactivation upregulates *Hes1* expression and induces some opposite phenotypes. To test this hypothesis, we crossed the ROSA-NICD mouse line with the Amhr2-cre to conditionally activate Notch1 (ca-Notch1) in ovarian somatic cells at P0 (Murtaugh et al., 2003). First, we checked whether NICD was upregulated in the ovary by Hes1 real-time PCR and immunohistochemistry in ca-Notch1 ovaries. We found that *Hes1* mRNA and protein levels were upregulated suggesting that NICD is activated (supplementary Figs. S1C and S2E). Then we examined the ca-Notch1 ovaries. Histological analysis showed large oocytes in the ca-Notch1 ovaries (Fig. 8A). In the ca-Notch1 ovaries, the average oocyte diameter showed a non-significant increase of around 20% (Fig. 8B). The number of oocytes show a non-significant decrease of about 20% in the ca-Notch1 ovaries (Fig. 8C and D). Meiosis labeled by Sycp3 did not change (data not shown). On the other hand, maturation of oocytes evaluated by the Kit staining was enhanced in ca-Notch1 ovaries by about 40% (Fig. 8E and G). Then we investigated different somatic markers. The number of pregranulosa cells stained by Foxl2 decreased to about 30% (Fig. 8F and H). The medula marker Ngfr increased in the ca-Notch1 (Fig. 8I). By contrast, the endothelial cell marker Pecam1 did not change compared to the control (data not shown). These results suggest that overactivation of Notch induces some opposite phenotypes to *Hes1* KO, namely *Hes1* expression, maturation of oocytes and higher number of pregranulosa cells.

Reduced fertility in ovaries with somatic Notch pathway gene alterations

Because of the defects in somatic *Hes1* and Notch mutants, we would also expect lower fertility. To test this hypothesis, we generated adult mutant females and crossed them to WT male mice. Fertility was evaluated by counting the number of pups. We found that somatic *Hes1* cKO showed a decrease of the pup number at different ages (Fig. 9A). Somatic ca-Notch1 also decreased the number of pups (Fig. 9B). The lower fertility in these mutants can be explained by the lower number of oocytes during fetal ovary development. It is possible that the quality of oocytes is also decreased in these mutants. To examine this possibility, we superovulated 11-months old control and mutant female animals and counted the percentage of normal oocytes with metaphase plate and polar body. In the *Hes1* cKO animals, there was a tendency to a lower number of oocytes, and the number of normal oocytes also decreased (supplementary

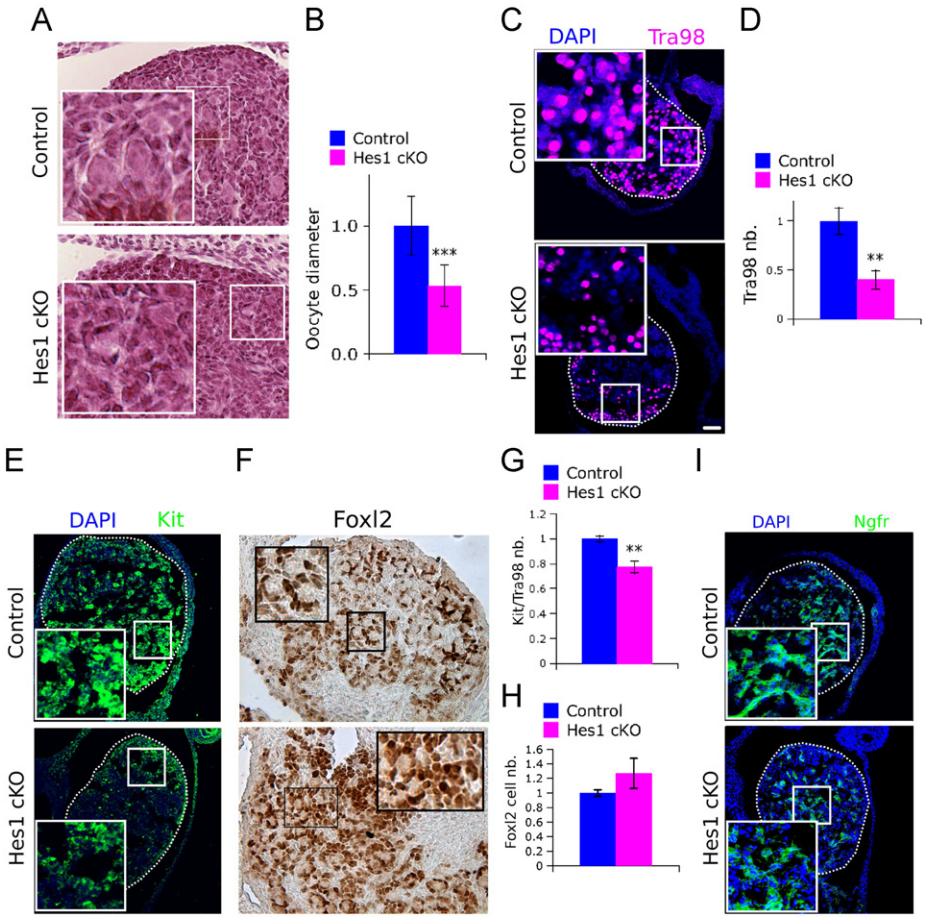

Fig. 7. Fewer and smaller oocytes in the somatic cell-specific *Hes1* cKO embryos. (A,B) Hematoxilin staining of paraffin sections and quantification. The average diameter of the cKO ovary is around 50% smaller than the control. (C,D) Immunofluorescence of the oocyte marker Tra98 and quantification. There is a 60% decrease of Tra98 positive oocyte number in the *Hes1* cKO. (E,G) Immunofluorescence of the mature oocyte marker Kit and quantification. The number of mature oocytes (Kit/Tra98 ratio) decreases by about 20%. (F,H) Immunohistochemistry of the pregranulosa cell maker Foxl2 and quantification. There is a non-significant increase of Foxl2 positive cells in the cKO ovaries. (I) Immunofluorescence of the medulla marker Ngfr. Ngfr decreases in the *Hes1* cKO ($n=2$). Boxed regions are enlarged in the corners. Scale bars: 50 μm; $^{**}P<0.01$, $^{***}P<0.001$.

Fig. S14). In the ca-Notch1 animals, we did not get any oocyte, so that it remains to be determined whether the total number or quality is changed in this mutant. These results show that appropriate expression levels of Notch pathway genes in ovarian somatic cells are important for fertility.

Discussion

There are currently few studies on the role of the Notch pathway for the mammalian ovary development. The bHLH transcription factor *Hes1* is an important downstream component of the Notch pathway, so that we examined ovaries deficient for the *Hes1* gene. We found that deletion of the *Hes1* gene in the ovarian somatic cells decreases oocyte size and number. *Hes1* deletion also decreased the number of oocytes with Kit protein, a growth marker and antiapoptotic gene. Higher apoptosis might be also explained by the upregulation of the proapoptotic gene *Inhbb*. Ovary culture with a Notch inhibitor decreases Hes1 promoter activity and protein levels and induces similar phenotypes as the *Hes1* deletion mutants. Conversely, overactivation of the Notch pathway in somatic cells upregulated *Hes1* mRNA and protein expression and induced some oposite phenotypes to the *Hes1* deletion mutant. Based on these results, we propose that in the ovary, *Hes1* expression is activated by the Notch pathway (supplementary Fig. S15). *Hes1* prevents apoptosis by a mechanism that might involve positive regulation of the Kit pathway and negative regulation of *Inhbb* gene expression (supplementary Fig. S15). Positive regulation of the Kit pathway by Hes1 might be also necessary for oocyte growth and maturation (supplementary Fig S15).

In invertebrates, it is well known that the Notch pathway is required in the ovary (Klusza and Deng, 2011). Also in mammals, chemical inhibition of Notch in neonatal ovaries affects the oocyte follicle formation (Trombly et al., 2009). *Hes1* is an important downstream effector of the Notch pathway, and we and others have found that *Hes1* is mainly expressed in ovarian somatic cells at fetal, neonatal and adult stages (Johnson et al., 2001; Trombly et al., 2009). Our results show that the Notch pathway and Hes1 mainly act in somatic cells since somatic cell-specific *Hes1* cKO showed similar phenotypes to conventional *Hes1* KO and DAPT treatment.

Hes1 belongs to the family of *Hes* genes (Kageyama et al., 2007). Genes of this family like *Hes1*, *Hes3*, *Hes5* and *Hey1* work redundantly in different contexts like the inner ear and intestine (Tateya et al., 2011; Ueo et al., 2012). In the mammalian ovary, other *Hes* genes are expressed in addition to *Hes1* (Trombly et al., 2009) (data not shown). Therefore, *Hes* family genes might carry out different functions redundantly in the ovary.

Meiosis is very important for oocyte development. It starts at around E13.5, and by P0 almost all oocytes have reached the dictyotene stage, which will be maintained until sexual maturity.

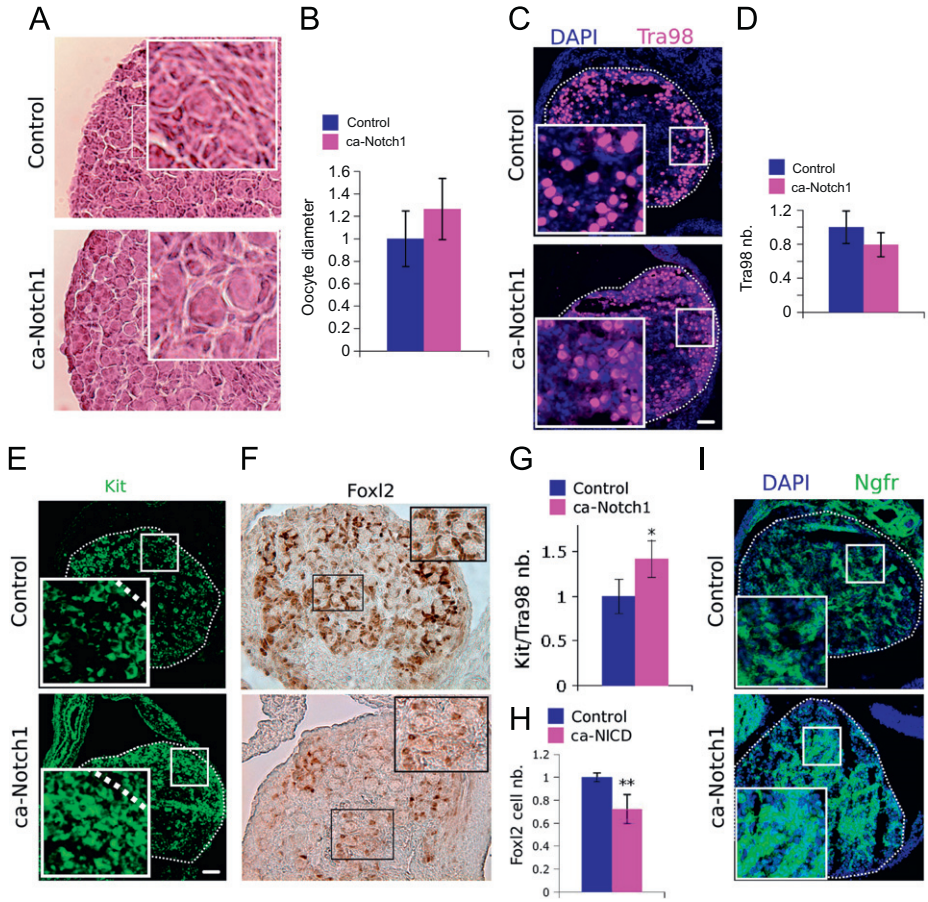

Fig. 8. More mature oocytes and fewer pregranulosa cells in somatic cell-specific ca-Notch1 ovaries. (A,B) Hematoxilin staining of paraffin sections and quantification. The average diameter of the ca-Notch1 oocytes shows a non-significant increase in the ca-Notch1 ovaries (B). (C,D) Immunofluorescence of the oocyte marker Tra98 and quantification. There is a non-significant 20% decrease of Tra98-positive oocyte number in the ca-Notch1 ovaries. (E,G) Immunofluorescence of the mature oocyte marker Kit and quantification. The number of mature oocytes (Kit/Tra98 ratio) increases by about 40%. (F,H) Immunohistochemistry of the pregranulosa cell marker Foxl2 and quantification. The number of Foxl2 positive cells decreases in the ca-Notch1 ovaries. (I) Immunofluorescence of the medulla marker Ngfr. Ngfr levels strongly increase. Boxed regions are enlarged in the corners. Scale bars: 50 μm; $^{**}P < 0.01$.

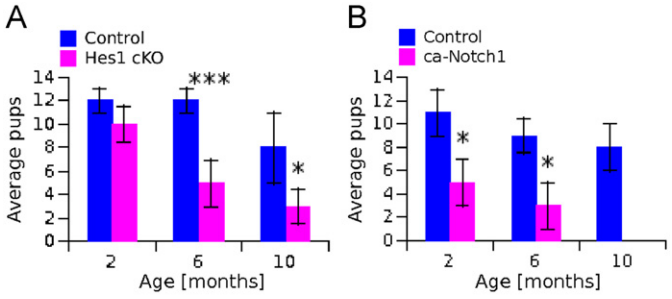

Fig. 9. Reduced fertility in ovaries with altered Notch pathway activity. The number of pups for control, somatic *Hes1* cKO (A) and somatic ca-Notch1 (B) female mice were counted. We found a decrease of the average number of pups in the mutant females.

A previous study found that the Notch gene *Lfng* showed decreased fertility and abnormal meiotic maturation in adult females (Hahn et al., 2005). In the *Hes1* KO ovaries, we did not find meiotic defects after spreading and labeling the chromosomes with Sycp3, suggesting that *Hes1* is not needed for meiotic maturation.

Apoptosis is a normal physiological process in oocytes around birth, when the oocyte number is reduced to about half (Ratts et al., 1995). We have found that Hes1 is required for oocyte survival, since we observe a decrease of oocytes in the *Hes1* KO. Furthermore, this requirement is non-cell autonomous since oocyte survival decreases in the somatic *Hes1* cKO mice.

The increase of apoptosis correlated with higher expression of the proapoptotic gene *Inhbb*, a member of the Tgfb family (supplementary Fig. S15). *Wnt4* mutation in the ovary increases Inhbb expression and apoptosis, but the apoptosis is reverted by simultaneous deletion of *Inhbb* and *Wnt4* alleles (Liu et al., 2010). One possibility is that higher *Inhbb* expression increases apoptosis in the *Hes1* KO ovaries. However, Inhbb is post-transcriptionally inhibited by Fst, whose expression is also increased in *Hes1* KO ovaries (Fig. 3C) (Phillips and de Kretser 1998). We do not know how Fst or Inhbb protein levels change in the Hes1 KO ovaries, so that we cannot conclude that *Inhbb* is responsible for the apoptosis phenotype. An experiment to prove the role of *Inhbb* in the apoptosis phenotype of the *Hes1* KO ovaries would be to delete the *Hes1* and *Inhbb* alleles simultaneously and check whether the apoptosis of germ cells is reverted.

The higher expression of *Inhbb* in the *Hes1* KO ovaries can be explained in two ways (supplementary Fig. S15). One explanation would be that the expression of *Wnt4* is decreased, which then results in higher expression of *Inhbb* (Liu et al., 2010). Another explanation would be that Hes1 represses the *Inhbb* promoter directly as shown in cultured cells here.

In the *Hes1* KO ovaries, *Fst* mRNA expression is upregulated, while *Wnt4* mRNA expression is decreased (supplementary Fig. S15). *Fst* expression was shown to be positively regulated by Wnt4 raising the question of how *Fst* expression is increased

(Yao et al., 2004; Ottolenghi et al., 2007). *Fst* mRNA expression is also positively regulated by *Foxl2* overexpression in granulosa-like cells (Kashimada et al., 2011). Moreover, most authors place Foxl2 and Wnt4 in independent pathways (Liu et al., 2010; Veitia, 2010). Therefore, higher Foxl2 levels could explain higher Fst mRNA expression in the *Hes1* KO ovary (supplementary Fig. S15).

Another pathway linked to ovarian apoptosis is the Kitl/Kit pathway, where the ligand Kitl in somatic cells activates the tyrosine kinase receptor Kit in the oocytes (Driancourt et al., 2000). During fetal development, a Kit antibody blocks the Kitl/Kit pathway and increases apoptosis (Reynaud et al., 2000; Doneda et al., 2002). This antiapoptotic effect of Kitl might be mediated by positive regulation of the antiapoptotic factor Bcl2 via the Phosphoinositide 3-kinase (PI3K) pathway (Jin et al., 2005). In the *Hes1* KO ovaries, there is lower *Kitl* and *Kit* expression, which might contribute to the apoptosis phenotype (supplementary Fig. S15).

The Kitl/Kit pathway also promotes follicle maturation and oocyte growth (Packer et al., 1994; Parrott and Skinner, 1999; Driancourt et al., 2000). *Kit* mutant mice show abnormal follicle maturation (John et al., 2009). For these reasons, lower *Kitl* and *Kit* expression might explain the smaller and more immature oocytes of *Hes1* KO ovaries. *Ngf* is also important for the follicle number, because *Ngf* KO ovaries show less primary and secondary follicles (Dissen et al., 2001). Therefore, lower Kit and Ngf levels in the *Hes1* KO ovaries might contribute to the smaller oocytes (Parrott and Skinner, 1999; Doneda et al., 2002; Dissen et al., 2001).

We have found that the number of pregranulosa cells and the area of endothelial cells increase at E15.5. Furthermore, proliferation is also increased at E15.5, and this correlates with a decrease of the expression of the cell cycle inhibitor Cdkn1c. These observations suggest that proliferation and differentiation are accelerated in the absence of Hes1, which could be explained if Hes1 slows down differentiation of somatic cells to prevent depletion of precursor cells at E15.5. In the nervous system, Hes1 is expressed in neural stem cells (Kageyama et al., 2008). In the absence of Notch signaling, neuronal differentiation is accelerated and as a consequence, neuronal stem cells become depleted (Imayoshi et al., 2010). In agreement with this explanation, we find that the marker of the precursors of pregranulosa cells Lhx9 is decreased at E18.5 (Mazaud et al., 2002).

The decrease of precursors of pregranulosa cells could explain why proliferation is decreased at E18.5. Another explanation would be the expression increase of the cell cycle inhibitors Cdkn1b and Gadd45g. *Cdkn1b* in the ovary is known to regulate cell proliferation, because ovaries without *Cdkn1b* produce more primary follicles (Rajareddy et al., 2007).

Previous reports have found that the female pregranulosa cell factor Foxl2 represses the male Sertoli cell marker Sox9 (Yao et al., 2006). However, we have found that in the Hes1 KO both genes are activated raising the question of why Sox9 is upregulated. One explanation would be that Sox9 is upregulated because Wnt4, another repressor of Sox9, is downregulated (Yao et al., 2006). Another explanation would be that Lhx9, a precursor of both Foxl2 and Sox9, is downregulated (Mazaud et al., 2002).

The Notch pathway is very important for fetal development of many organs, including invertebrate ovaries, but its role in murine ovarian development is not well understood. Therefore, our findings provide new insights into the mammalian ovary development.

Acknowledgments

We would like to thank Richard Behringer for the Amhr2cre mice and Kelly E. Mayo for the Inhbb promoter luciferase reporter. This work was supported by Grants-in-aid from the Ministry of Education, Culture, Sports, Science and Technology of Japan.

Appendix A. Supporting information

Supplementary data associated with this article can be found in the online version at http://dx.doi.org/10.1016/j.ydbio.2012.12.015.

References

Andersson, E.R., Sandberg, R., Lendahl, U., 2011. Notch signaling: simplicity in design, versatility in function. Development 138, 3593–3612.
Dissen, G.A., Romero, C., Hirshfield, A.N., Ojeda, S.R., 2001. Nerve growth factor is required for early follicular development in the mammalian ovary. Endocrinology 142, 2078–2086.
Doneda, L., Klinger, F.-G., Larizza, L., Felici, M.D., 2002. KL/KIT co-expression in mouse fetal oocytes. Int. J. Dev. Biol. 46, 1015–1021.
Driancourt, M.A., Reynaud, K., Cortvrindt, R., Smitz, J., 2000. Roles of KIT and KIT LIGAND in ovarian function. Rev. Reprod. 5, 143–152.
Dykema, J.C., Mayo, K.E., 1994. Two messenger ribonucleic acids encoding the common beta B-chain of inhibin and activin have distinct 5'-initiation sites and are differentially regulated in rat granulosa cells. Endocrinology 135, 702–711.
Ghafari, F., Gutierrez, C.G., Hartshorne, G.M., 2007. Apoptosis in mouse fetal and neonatal oocytes during meiotic prophase one. BMC Dev. Biol. 7, 87.
Hahn, K.L., Johnson, J., Beres, B.J., Howard, S., Wilson-Rawls, J., 2005. Lunatic fringe null female mice are infertile due to defects in meiotic maturation. Development 132, 817–828.
Han, H., Tanigaki, K., Yamamoto, N., Kuroda, K., Yoshimoto, M., Nakahata, T., Ikuta, K., Honjo, T., 2002. Inducible gene knockout of transcription factor recombination signal binding protein-J reveals its essential role in T versus B lineage decision. Int. Immunol. 14, 637–645.
Hopfer, O., Zwahlen, D., Fey, M.F., Aebi, S., 2005. The Notch pathway in ovarian carcinomas and adenomas. Br. J. Cancer 93, 709–718.
Imayoshi, I., Sakamoto, M., Yamaguchi, M., Mori, K., Kageyama, R., 2010. Essential roles of Notch signaling in maintenance of neural stem cells in developing and adult brains. J. Neurosci. 30, 3489–3498.
Imayoshi, I., Shimogori, T., Ohtsuka, T., Kageyama, R., 2008. Hes genes and neurogenin regulate non-neural versus neural fate specification in the dorsal telencephalic midline. Development 135, 2531–2541.
Ishibashi, M., Ang, S.L., Shiota, K., Nakanishi, S., Kageyama, R., Guillemot, F., 1995. Targeted disruption of mammalian hairy and Enhancer of split homolog-1 (HES-1) leads to up-regulation of neural helix-loop-helix factors, premature neurogenesis, and severe neural tube defects. Genes Dev. 9, 3136–3148.
Jamin, S.P., Arango, N.A., Mishina, Y., Hanks, M.C., Behringer, R.R., 2002. Requirement of Bmpr1a for Müllerian duct regression during male sexual development. Nat. Genet. 32, 408–410.
Jin, X., Han, C.-S., Yu, F.-Q., Wei, P., Hu, Z.-Y., Liu, Y.-X., 2005. Anti-apoptotic action of stem cell factor on oocytes in primordial follicles and its signal transduction. Mol. Reprod. Dev. 70, 82–90.
John, G.B., Shidler, M.J., Besmer, P., Castrillon, D.H., 2009. Kit signaling via PI3K promotes ovarian follicle maturation but is dispensable for primordial follicle activation. Dev. Biol. 331, 292–299.
Johnson, J., Espinoza, T., McGaughey, R.W., Rawls, A., Wilson-Rawls, J., 2001. Notch pathway genes are expressed in mammalian ovarian follicles. Mech. Dev. 109, 355–361.
Kageyama, R., Ohtsuka, T., Kobayashi, T., 2007. The Hes gene family: repressors and oscillators that orchestrate embryogenesis. Development 134, 1243–1251.
Kageyama, R., Ohtsuka, T., Shimojo, H., Imayoshi, I., 2008. Dynamic Notch signaling in neural progenitor cells and a revised view of lateral inhibition. Nat. Neurosci. 11, 1247–1251.
Klusza, S., Deng, W.-M., 2011. At the crossroads of differentiation and proliferation: precise control of cell-cycle changes by multiple signaling pathways in Drosophila follicle cells. Bioessays 33, 124–134.
Kobayashi, T., Mizuno, H., Imayoshi, I., Furusawa, C., Shirahige, K., Kageyama, R., 2009. The cyclic gene Hes1 contributes to diverse differentiation responses of embryonic stem cells. Genes Dev. 23, 1870–1875.
Liu, C.-F., Parker, K., Yao, H.H.-C., 2010. WNT4/beta-catenin pathway maintains female germ cell survival by inhibiting activin beta B in the mouse fetal ovary. PLoS One 5, e10382.
Lomelí, H., Ramos-Mejía, V., Gertsenstein, M., Lobe, C.G., Nagy, A., 2000. Targeted insertion of Cre recombinase into the TNAP gene: excision in primordial germ cells. Genesis 26, 116–117.
Masamizu, Y., Ohtsuka, T., Takashima, Y., Nagahara, H., Takenaka, Y., Yoshikawa, K., Okamura, H., Kageyama, R., 2006. Real-time imaging of the somite segmentation clock: revelation of unstable oscillators in the individual presomitic mesoderm cells. Proc. Natl. Acad. Sci. USA 103, 1313–1318.
Mazaud, S., Oréal, E., Guigon, C.J., Carré-Eusèbe, D., Magre, S., 2002. Lhx9 expression during gonadal morphogenesis as related to the state of cell differentiation. Gene Expr. Patterns 2, 373–377.

Murtaugh, L.C., Stanger, B.Z., Kwan, K.M., Melton, D.A., 2003. Notch signaling controls multiple steps of pancreatic differentiation. Proc. Natl. Acad. Sci. USA 100, 14920–14925.

Ottolenghi, C., Pelosi, E., Tran, J., Colombino, M., Douglass, E., Nedorezov, T., Cao, A., Forabosco, A., Schlessinger, D., 2007. Loss of Wnt4 and Foxl2 leads to female-to-male sex reversal extending to germ cells. Hum. Mol. Genet. 16, 2795–2804.

Packer, A.I., Hsu, Y.C., Besmer, P., Bachvarova, R.F., 1994. The ligand of the c-kit receptor promotes oocyte growth. Dev. Biol. 161, 194–205.

Parrott, J.A., Skinner, M.K., 1999. Kit-ligand/stem cell factor induces primordial follicle development and initiates folliculogenesis. Endocrinology 140, 4262–4271.

Pepling, M.E., Spradling, A.C., 1998. Female mouse germ cells form synchronously dividing cysts. Development 125, 3323–3328.

Phillips, D.J., de Kretser, D.M., 1998. Follistatin: a multifunctional regulatory protein. Front. Neuroendocrinol. 19, 287–322.

Rajareddy, S., Reddy, P., Du, C., Liu, L., Jagarlamudi, K., Tang, W., Shen, Y., Berthet, C., Peng, S.L., Kaldis, P., Liu, K., 2007. p27kip1 (Cyclin-dependent kinase inhibitor 1B) controls ovarian development by suppressing follicle endowment and activation and promoting follicle atresia in mice. Mol. Endocrinol. 21, 2189–2202.

Ratts, V.S., Flaws, J.A., Kolp, R., Sorenson, C.M., Tilly, J.L., 1995. Ablation of bcl-2 gene expression decreases the numbers of oocytes and primordial follicles established in the post-natal female mouse gonad. Endocrinology 136, 3665–3668.

Reynaud, K., Cortvrindt, R., Smitz, J., Driancourt, M.A., 2000. Effects of Kit Ligand and anti-Kit antibody on growth of cultured mouse preantral follicles. Mol. Reprod. Dev. 56, 483–494.

Shimojo, H., Ohtsuka, T., Kageyama, R., 2008. Oscillations in notch signaling regulate maintenance of neural progenitors. Neuron 58, 52–64.

Speed, R.M., 1982. Meiosis in the foetal mouse ovary. I. An analysis at the light microscope level using surface-spreading. Chromosoma 85, 427–437.

Tateya, T., Imayoshi, I., Tateya, I., Ito, J., Kageyama, R., 2011. Cooperative functions of Hes/Hey genes in auditory hair cell and supporting cell development. Dev. Biol. 352, 329–340.

Tang, H., Brennan, J., Karl, J., Hamada, Y., Raetzman, L., Capel, B., 2008. Notch signaling maintains Leydig progenitor cells in the mouse testis. Development 135, 3745–3753.

Trombly, D.J., Woodruff, T.K., Mayo, K.E., 2009. Suppression of Notch signaling in the neonatal mouse ovary decreases primordial follicle formation. Endocrinology 150, 1014–1024.

Uda, M., Ottolenghi, C., Crisponi, L., Garcia, J.E., Deiana, M., Kimber, W., Forabosco, A., Cao, A., Schlessinger, D., Pilia, G., 2004. Foxl2 disruption causes mouse ovarian failure by pervasive blockage of follicle development. Hum. Mol. Genet. 13, 1171–1181.

Ueo, T., Imayoshi, I., Kobayashi, T., Ohtsuka, T., Seno, H., Nakase, H., Chiba, T., Kageyama, R., 2012. The role of Hes genes in intestinal development, homeostasis and tumor formation. Development 139, 1071–1082.

Veitia, R.A., 2010. FOXL2 versus SOX9: a lifelong battle of the sexes. Bioessays 32, 375–380.

Wang, M., Wu, L., Wang, L., Xin, X., 2010. Down-regulation of Notch1 by gamma-secretase inhibition contributes to cell growth inhibition and apoptosis in ovarian cancer cells A2780. Biochem. Biophys. Res. Commun. 393, 144–149.

Waters, K.A., Reinke, V., 2011. Extrinsic and intrinsic control of germ cell proliferation in *Caenorhabditis elegans*. Mol. Reprod. Dev. 78, 151–160.

Yao, H.H.C., Matzuk, M.M., Jorgez, C.J., Menke, D.B., Page, D.C., Swain, A., Capel, B., 2004. Follistatin operates downstream of Wnt4 in mammalian ovary organogenesis. Dev. Dyn. 230, 210–215.

Yao, H.H.-C., Aardema, J., Holthusen, K., 2006. Sexually dimorphic regulation of inhibin beta B in establishing gonadal vasculature in mice. Biol. Reprod. 74, 978–983.